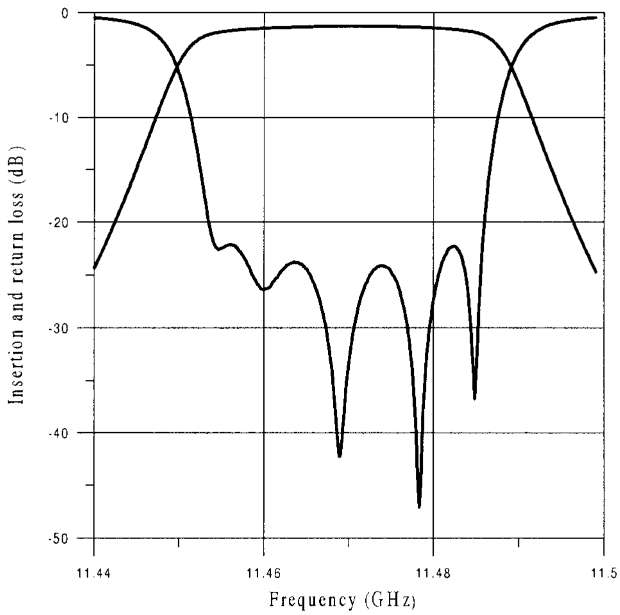

Figure 3 Measured performance of a *Ku*-band five-pole filter

ing to an unloaded quality factor of 2700. In this case, we have achieved a threefold increase of the quality factor.

The last example we discuss is a seven-pole filter (bandwidth 90 MHz) centered at 7.066 GHz. This filters uses standard WR 137 input/ output connections, and has been manufactured using resonators of square cross section ($A = B = 40$ mm). The transition between the input of the filter and the standard waveguide has been implemented with a stepped transformed. The filter was first designed as a simple inductive filter [2], and was then optimized, including the transformer, using an efficient full-wave algorithm [3]. The measured response of the filter is shown in Figure 4. The minimum value of insertion loss is 0.273 dB, which corresponds to an unloaded quality factor of 13,600. The same filter using the standard waveguide height (15.85 mm) would give a minimum insertion loss of 0.55 dB, resulting in an unloaded quality factor of about 6750. We have therefore doubled the quality factor.

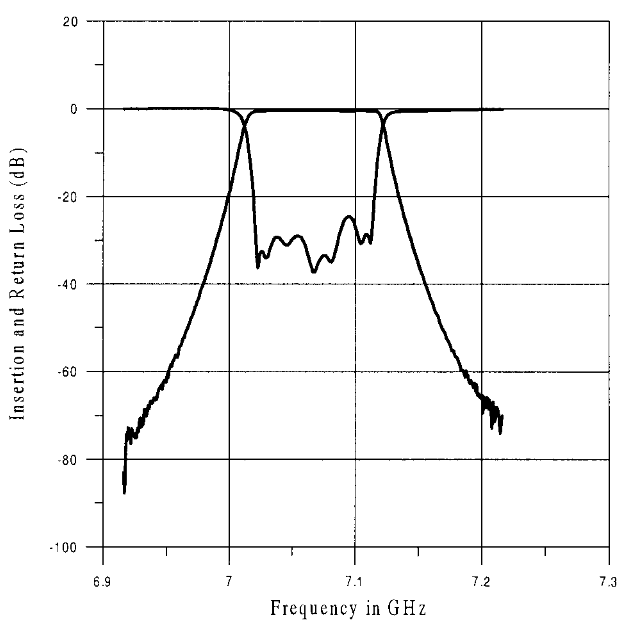

Figure 4 Measured performance of a seven-pole *C*-band filter

IV. CONCLUSION

In this paper, we discuss a low-cost technique for manufacturing low-loss inductive-window microwave filters in rectangular waveguides. The basic concept is indeed very simple, and consists of increasing the height of the rectangular waveguide resonators. The effectiveness of this technique has been demonstrated, discussing the measured results of a number of filters. A threefold maximum increase of the unloaded quality factor has been demonstrated. Although the use of this technique requires the filters to be longer, the inherent simplicity and achieved reduction in insertion loss make it very attractive for all applications where RF power loss must be minimized.

REFERENCES

1. G. Matthaei, L. Young, and E.M.T. Jones, Microwave filters, impedance matching networks, and coupling structures, Artech House, Dedham, MA, 1980.
2. M. Guglielmi, G. Gheri, M. Calamia, and G. Pelosi, Rigorous multimode network numerical representation of inductive steps, IEEE Trans Microwave Theory Tech 42 (1994).
3. R. Sorrentino, F. Alessandri, M. Mongiardo, G. Avitabile, and L. Roselli, Full-wave modeling of via hole grounds in microstrip by three-dimensional mode matching technique, IEEE Trans Microwave Theory Tech 40 (1992), 2228–2234.

OPTICALLY TUNABLE MILLIMETER-WAVE ATTENUATOR BASED ON LAYERED STRUCTURES

Sangil Lee,[1] Yasuo Kuga,[1] and Ruth Ann Mullen[2]
[1] Department of Electrical Engineering
University of Washington
Seattle, Washington 98195-2500
[2] Nextlink
Bellevue, Washington 98004

Received 19 April 2000

ABSTRACT: *A new type of optically controllable, millimeter-wave (MMW) attenuator based on high-resistivity (high-R) silicon (Si) wafers and a layered structure is developed. A high-R float-zone Si wafer is a lossless dielectric material at microwave frequency without optical excitation. When an Si wafer is optically excited, free carriers are generated, and the Si wafer becomes a lossy dielectric. This property is combined with a layered structure to develop a simple optically tunable MMW attenuator. A more than 20 dB attenuation with a 10% bandwidth of the center frequency is obtained at W-band. The proposed structure is useful for developing low-cost attenuators and switches in the MMW region.* © 2000 John Wiley & Sons, Inc. Microwave Opt Technol Lett 27: 9–13, 2000.

Key words: *millimeter wave; optically tunable attenuator; layered structure; high-resistivity silicon; optical excitation*

I. INTRODUCTION

The attenuators, switches, and tunable windows are an important part of microwave and MMW systems. Although low-cost devices are presently available at microwave frequencies, attenuators and switches at MMW frequencies (75–240 GHz) are still expensive. A layered structure with high-R Si wafers whose dielectric constant can be changed with laser excitation is used to create the tunable transmission characteristics. Layered structures are frequently used as microwave-frequency-selective surfaces. However, these structures usually have fixed transmission characteristics, and it is difficult to control the pass- and stopband responses without changing the physical spacing or surface patterns.

In this paper, we will describe a simple attenuator whose responses can be controlled by light. The device is based on a layered structure with two Si plates and an air gap between them. Our design goal is to obtain an attenuation value greater than 20 dB with less than 0.1 W/cm^2 light excitation. The complex dielectric constants of a high-R Si wafer are measured with and without laser excitation from 75 to 110 GHz. The transmission characteristics of layered structures are simulated using the measured dc. A simple layered structure is constructed and tested at W-band. A better than 20 dB attenuation with a 10% bandwidth of the center frequency is obtained at W-band. Two different attenuators are proposed.

II. DIELECTRIC CONSTANT OF A HIGH-R SI WAFER WITH AND WITHOUT EXCITATION

Our proposed device is based on a change of complex dielectric constant with and without light excitation. Although the dielectric constant of high-R Si wafers can be readily obtained from manufacturers, we were unable to find the complex dielectric constant of an optically excited Si wafer [1–4]. Therefore, the first task was to measure the dielectric constant of a high-R Si wafer with and without light excitation. The technique to measure the dielectric constant of lossless or slightly lossy materials at microwave frequency is well known, and accurate results can be obtained easily [5]. However, the measurement of the complex dielectric constants of lossy materials such as an optically exited Si wafer is much more difficult, and a robust data inversion method must be employed [6, 7]. Based on our experience with the BeO–SiC composite materials which are commonly used for controlling the cavity-Q in high-power microwave tubes, we knew that the reflection (S_{11}) measurement is susceptible to a measurement error [7]. Therefore, the transmission (S_{21}) experiment was conducted using a high-R float-zone Si wafer (thickness: 0.55 mm, n/Ph doped, resistivity > 1000 $\Omega \cdot$ cm, orientation: ⟨100⟩) in the frequency range from 75 to 110 GHz.

The Si wafer is placed in front of an open-ended MMW waveguide, and the transmitted signals are measured with a receiving horn antenna. The Si wafer is optically excited with a multiline (blue–green) CW Ar laser at a predetermined energy density. Figure 1 shows S_{21} data with and without light excitation. The *thru* calibration is used, and 0 dB corresponds to a free-space measurement without an Si wafer. The measured S_{21} is related to the dielectric constant through Eq. (1) [6, 7]. The iterative method with genetic algorithms (GAs) is used to extract the complex dc from Eq. (1) [7, 8].

$$S_{21}(\omega) = \frac{z(1-\Gamma^2)}{1-\Gamma^2 z^2}$$

$$Z = \exp(-\gamma L), \qquad \Gamma = \frac{\gamma_0 - \gamma}{\gamma_0 + \gamma}$$

$$\gamma = j\sqrt{\frac{\omega^2 \varepsilon_r}{C_0^2}}, \qquad \gamma_0 = j\sqrt{\frac{\omega^2}{C_0^2}} \qquad (1)$$

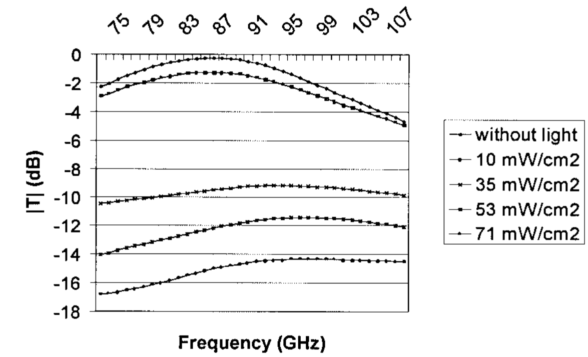

Figure 1 Transmission coefficient (S_{21}) measurements in the air with an open-ended waveguide

where $\varepsilon_r = \varepsilon_r' - j\varepsilon_r''$, $j = \sqrt{-1}$, ω is the angular frequency, γ_0 is the propagation constant in the air, γ is the propagation constant in the material, L is the sample thickness, $\mu = \mu_0$, and $C_0 = C_{\text{vacuum}}$.

Figure 2 shows some of the measured complex dielectric constants as a function of frequency and the laser power density. A pure Si wafer is a low-loss dielectric material, and the real part of the complex dielectric constant is quoted as 11.6, but the imaginary part has a range from 0.046 to 464 at 35 GHz corresponding to its resistivity (1000–0.1 $\Omega \cdot$ cm) [1]. However, in case of a high-R Si wafer, the resistivity is usually greater than 1000 $\Omega \cdot$ cm; thus, the imaginary part of the complex dielectric constant is less than 0.04 at 35 GHz. Our measured values without light at MMW have a real part between 10 and 12, and the imaginary part is very small. When the Si wafer is excited with light, the real part shows no significant change. However, the imaginary part increases as the light intensity increases, as shown in Figure 2. This is consistent with the expected increase of free carriers in an Si wafer which has an indirect bandgap energy (1.12 eV), and light with a wavelength less than 1.1 μm should be able to excite free carriers. The conductivity is given by $\sigma = N_0 q_e \mu_s$, where q_e is the electron charge, μ_s is the mobility, and N_0 is the number of free carriers. Although the maximum carrier density N_0 can be up to 10^{18} for a high-R Si wafer with the CW laser [4], our results indicate that N_0 is approximately 5×10^{16}, which is much smaller than that in our experiment. Although the absorption depth of Si at 500 nm wavelength is approximately 1 μm, the electron diffusion length is 70 mm, which is much greater than the wafer thickness (0.55 mm) [4]. Therefore, we will assume that the free carriers are distributed uniformly within the illuminated region.

III. TRANSMISSION CHARACTERISTICS OF LAYERED STRUCTURES

The transmission characteristics shown in Figure 1 clearly reveal the feasibility of using the high-R Si wafer as a tunable attenuator. However, the level of attenuation and applicable bandwidth are not sufficient to be used as a practical device. To improve the attenuation and frequency characteristics, we constructed a layered structure with two high-R silicon wafers separated by 0.6 mm, as shown in Figure 3. Although the structure shown in Figure 3 allows light excitation for both sides from the gap to maximize the photon utilization, in this experiment, we illuminated the layered structure from one side, as shown in Figure 3.

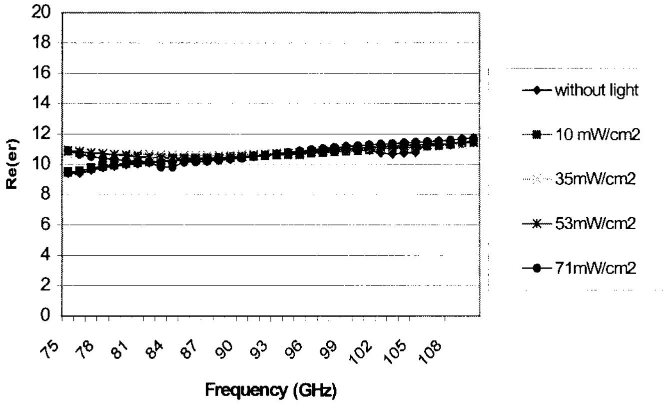

(a)

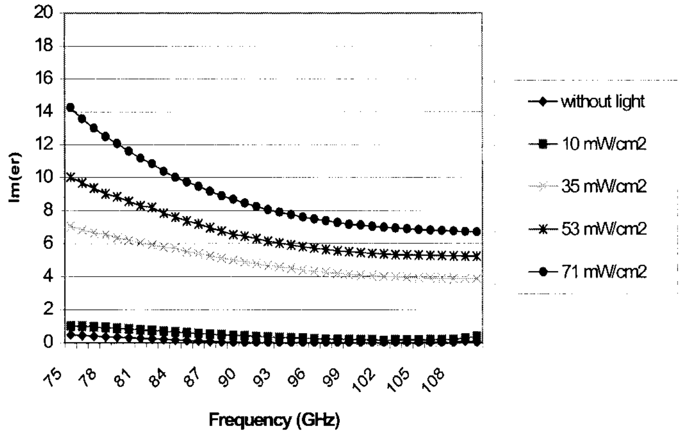

(b)

Figure 2 Measured dielectric constants with laser beam diameter = 0.6 cm. (a) Real part. (b) Imaginary part

The transmission coefficient T of a two-Si wafer structure can be obtained using an $ABCD$ matrix of three layers as [9]

$$T = \frac{2}{(A + B/Z_t + Z_{\text{in}} \cdot (C + D/Z_t))}$$

$$\begin{aligned}[ABCD] = {} & [A_1B_1C_1D_1\text{: silicon layer 1}] \\ & \cdot[A_2B_2C_2D_2\text{: air between}] \\ & \cdot[A_3B_3C_3D_3\text{: silicon layer 2}] \qquad (2)\end{aligned}$$

where Z_{in}, Z_t is the wave impedance at the incident and transmitted layer, and A_m, B_m, C_m, D_m are the matrix components of the mth $ABCD$ matrix. Figure 4(a) shows the estimated transmission coefficient T with and without light excitation. The constant values for both real and imaginary parts are assumed for this calculation. Our design goal is to obtain an attenuation value greater than 20 dB with less than 0.1 W/cm^2 light excitation. To achieve more than 20 dB attenuation, however, the imaginary part of the complex dielectric constant should be 18, which corresponds to over 0.35 W/cm^2 laser power density. The expected passband bandwidth is better than 10% of the center frequency at $f_o = 85$ GHz.

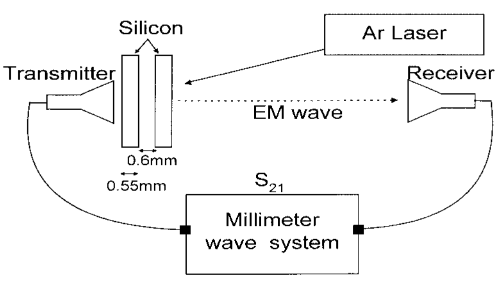

Figure 3 Millimeter-wave measurement setup for a layered structure

Figure 4(b) shows experimental results when only one side is optically excited. Without light excitation, the transmission characteristics are very similar to the simulation results shown in Figure 4(a). The attenuation characteristics with 0.35 W/cm^2 are similar to the simulation using $\varepsilon_r = 12 - j18$. The layered structure also provides more than 10 GHz bandwidth at 85 GHz, which corresponds to better than 10% of the center frequency. Although the experiment was performed with a single-side illumination of an Si wafer, we were able to achieve a desired value of 20 dB attenuation with 0.35 W/cm^2 power. We expect that the attenuation can be increased if both Si wafers are excited from inside the gap.

IV. PROPOSED MMW ATTENUATORS

We have demonstrated that a low-cost optically tunable attenuator can be constructed with a high-R Si wafer. However, the practical device must be designed to maximize the attenuation value with the least amount of optical power. Two proposed devices are an optical window [Fig. 5(a)] and a waveguide MMW attenuator [Fig. 5(b)]. In both cases, the laser light is guided into the gap, and a uniform illumination must be created using a diffuser such as rough surfaces or light-scattering particles. Currently, we are developing both

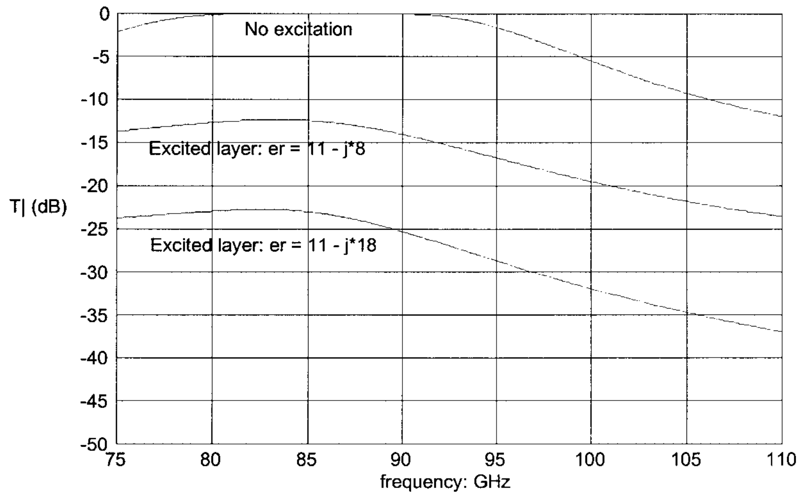

(a)

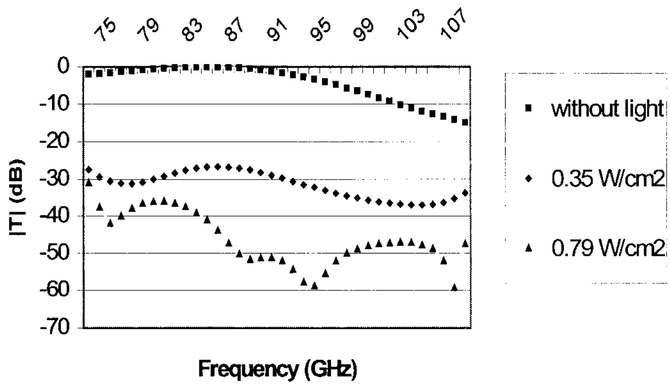

(b)

Figure 4 Transmission coefficient (S_{21}) with a two-layered structure. (a) Simulated. (b) Measured

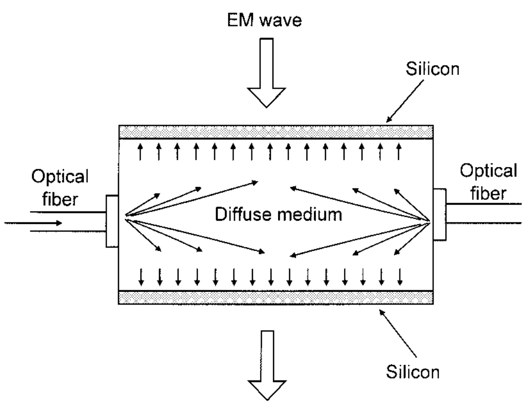

(a)

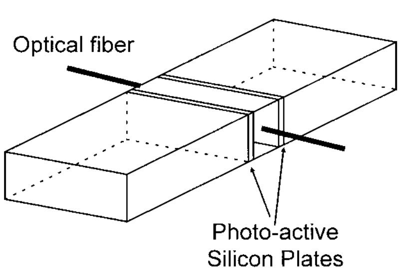

(b)

Figure 5 Proposed models for an optically tunable attenuator based on a layered structure in the millimeter-wave range. (a) Optical window MMW attenuator. (b) Waveguide MMW attenuator

devices at *W*-band. A required light intensity for the *W*-band waveguide attenuator will be approximately 0.1 W to obtain better than 20 dB attenuation based on the waveguide cross section of 2.54 mm × 1.27 mm.

The transmission characteristics of a layered structure in a waveguide structure are different from those of free space. For a rectangular waveguide, the TE_{10} mode is the dominant mode, and the transmission coefficient must be calculated using the propagation constant of the TE_{10} mode. Figure 6 shows the transmission characteristics of the *W*-band waveguide attenuator described in Figure 5(b). The overall characteristics are similar to those of the free-space transmission case. With $\varepsilon_r = 11 - j7$ of the activated Si layer, which corresponds to 0.07 W/cm^2 laser power, a single-layer activation has only 13 dB attenuation at 85 GHz. However, if both layers are activated, the proposed device shows more than 25 dB attenuation.

V. CONCLUSIONS

Optically tunable attenuators based on a layered structure are demonstrated at *W*-band. The measured data agree with simulations using the complex dielectric constant of an Si wafer which was obtained experimentally. We believe that the proposed device is useful for low-cost waveguide attenuators and switches. The required optical power is expected to be about 0.1 W/cm^2 to obtain more than 20 dB attenuation at *W*-band. The experiments were conducted with float-zone Si wafers which were available in our laboratory. We have not tested other float-zone high-*R* Si wafers such as *p*-type doped

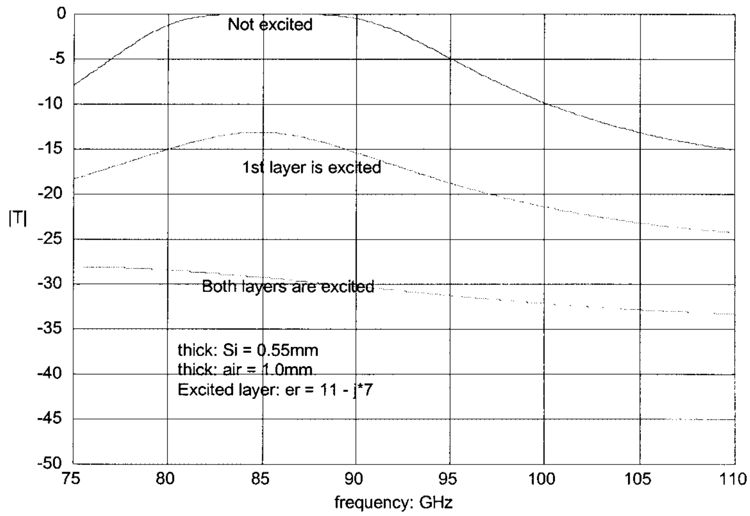

Figure 6 Transmission characteristics in the waveguide structure

materials and very high-R Si wafers (greater than 10,000 $\Omega \cdot$ cm). Another important consideration is switching speed. It is known that the carrier lifetime in Si is relatively long, and this may limit the speed of the proposed device [10]. However, a published report using an Nd–YAG pulse laser excitation shows a much faster switching time than the one expected from the carrier lifetime [11, 12]. Further studies will be conducted with a pulse diode laser.

REFERENCES

1. J. Musil and F. Zacek, Microwave measurements of complex permittivity by free space methods and their applications, Elsevier, Amsterdam, The Netherlands, 1986.
2. Z. Wang and Y. Chu, Use of microwave photoconductivity to measure semiconductor properties, Solid-State Electron 34 (1991), 735–740.
3. A. Sanders and M. Kunst, Characterization of silicon wafers by transient microwave photoconductivity, Solid-State Electron 34 (1991), 1007–1015.
4. R. Edwards, W. Nunnally, D. Brian, C. Miller, and L. Robinett, Investigation of photoconductive silicon as a reconfigurable antenna, SPIE, Smart sensing, processing, and instrument 1918 (1993), 344–353.
5. HP product note 8510-3.
6. J. Baker-Jarvis and E.J. Vanzura, Improved technique for determining complex permittivity with the transmission/reflection method, IEEE Trans 38 (1990), 1096–1101.
7. S. Lee and Y. Kuga, Complex dielectric constant measurements and model comparison of lossy dielectric materials, 2000 IEEE AP-S Int Symp, Salt Lake City, UT, July 2000.
8. D.E. Goldberg, Genetic algorithms in search, optimization, and machine learning, Addison-Wesley, Reading, MA, 1989.
9. A. Ishimaru, Electromagnetic wave propagation, radiation, and scattering, Prentice-Hall, Englewood Cliff, NJ, 1991.
10. J. Freeouf, N. Brasiau, and M. Wittmer, Lifetime measurements on silicon-on-insulator wafers, Appl Phys Lett 63 (1993), 189–190.
11. A. DeFonzo and C. Lutz, Optoelectronic transmission and reception of ultrashort electrical pulses, Appl Phys Lett 51 (1987), 212–214.
12. Y. Pastol, G. Arjavalingam, J. Halbout, and G. Kopcsay, Coherent broadband microwave spectroscopy using picosecond optoelectronic antennas, Appl Phys Lett 54 (1989), 307–309.

A HIERARCHICAL FAST-MULTIPOLE METHOD FOR STRATIFIED MEDIA

Y. C. Pan[1] and W. C. Chew[1]
[1] Center for Computational Electromagnetics
Department of Electrical and Computer Engineering
University of Illinois
Urbana, Illinois 61801-2991

Received 7 April 2000

ABSTRACT: *An efficient, static, fast-multipole method (FMM)-based algorithm is presented in this paper for the evaluation of the parasitic capacitance of 3-D microstrip signal lines above stratified dielectric media. A modified tree structure is used to perform the multilevel outgoing-to-local multipole translations. The algorithm, only marginally more expensive than the free-space FMM, retains its O(N) computational cost and memory use, where N is the number of conductor patches.*
 Microwave Opt Technol Lett 27: 13–17, 2000.

Key words: *static fast-multipole method; stratified dielectric media*

1. INTRODUCTION

A static multilayer FMM algorithm [1] was developed recently by Pan, Chew, and Wan that utilizes the image multipole expansions to account for the effect of stratified dielectric media. In that approach, most of the outgoing-to-local multipole translations are performed using interpolated translation functions. The use of interpolation drastically reduced the efficiency of their method. In this paper, we will use a modified tree structure for the image sources in conjunction with the free-space FMM tree structure to achieve a much improved static multilayer FMM algorithm.

2. MULTILEVEL FREE-SPACE FMM

To facilitate a good understanding of the new multilayer FMM algorithm, we will describe the free-space FMM [2, 3] in detail.

Contract grant sponsor: Air Force Office of Scientific Research
Contract grant number: MURI Grant F49620-96-1-0025
Contract grant sponsor: Intel Corporation